



Interferon Tau Is a Potent Oral Agent against SARS-CoV-2 Infection

Wanjin Tang¹, Xiaojun Liu¹, Fuller W Bazer² and George Zhang^{1*}

¹Southlake Pharmaceuticals, Inc, 125 Cambridge Park Drive, Cambridge, USA

²Department of Animal Science, Texas A&M University, College Station, Texas, USA

Abstract

To combat the ongoing COVID-19 pandemic, effective, safe, and broad-spectrum oral therapeutics are still in high demand [1]. Here we demonstrate, for the first time, that Interferon tau (IFN- τ) is highly potent in inhibiting SARS-CoV-2 infected Vero and Calu-3 cells, and it also improved outcomes in BALB/c mice infected with mouse-adapted SARS-CoV-2. In a Cytopathic Effect (CPE) assay *in vitro*, IFN- τ potently inhibited the SARS-CoV-2 activity with an IC₅₀ of 2.1 nM, which is ~1,000x more potent than the reference agents evaluated in the same assay, including Remdesivir, Chloroquine, Hydroxychloroquine, Aloxistatin, and Interferon Lambda (λ). *In vivo*, IFN- τ demonstrated oral efficacy in alleviating symptoms of mice infected by SARS-CoV-2 virus and decreased viral loads. Further, IFN- τ has a superior safety profile over other Type I interferons as demonstrated by pre-clinical animal studies as well as clinical studies reported in literature. In sum, we report here that IFN- τ is a potent oral agent against SARS-CoV-2 virus *in vitro* and *in vivo*, and may be further developed as an alternative treatment option in the battle against COVID-19 pandemic.

Introduction

The global outbreak of COVID-19 pandemic started about 4 years ago has severely compromised the health and daily life of general public and hampered economic growth. In addition to the development of an effective, safe, and lasting vaccine, there is a strong demand for effective, safe, and broad-spectrum oral therapeutics for treating infected patients. Various antiviral agents are under investigation or approved for treating the viral infection. In December 2021, FDA issued EUAs for two oral agents (Molnupiravir and Paxlovid) for the treatment of mild-to-moderate COVID-19 infection. (<https://www.fda.gov/news-events/press-announcements/coronavirus-covid-19-update-fda-authorizes-additional-oral-antiviral-treatment-covid-19>; <https://www.fda.gov/news-events/press-announcements/coronavirus-covid-19-update-fda-authorizes-first-oral-antiviral-treatment-covid-19>). Both drugs can be conveniently taken orally for treating COVID-19 infection, but some undesirable side effects and limitations to use these drugs have been reported [2,3]. Several other oral agents, such as Hydroxychloroquine or Chloroquine, which were previously thought or proclaimed to be effective against COVID-19, have since been shown to have minimal effects or may even be harmful [4,5]. Thus, effective, safe

and broad-spectrum oral treatments are still in high demand in the battle against COVID-19 pandemic.

Interferons (IFNs) are small glycoproteins secreted by eukaryotic cells to fight against viral infection. There are three classes of IFNs according to their different immunological and biological properties: types I, II and III interferons. Interferon tau (IFN- τ) is a member of the type I Interferon (IFN) family and is a novel pregnancy recognition signal secreted by mononuclear trophoblast cells of ruminant conceptuses during the first 3 to 4 weeks of pregnancy. In sheep, IFN- τ induces Interferon Regulatory Factor 1 (IRF2) that silences expression of receptors for estradiol and oxytocin so that uterine epithelial cells do not secrete oxytocin-dependent pulses of prostaglandin F-2 alpha. These pulses would regress corpora lutea on the ovaries that are required to produce progesterone essential for establishment and maintenance of pregnancy [6]. There is no functionally active human analog of IFN- τ . Within the type I IFN family, IFN- τ is mostly similar to IFN- ω (ω) with about 70% Amino Acid (AA) identity whereas it has about 50% AA identity with IFN- α and about 25% AA identity with IFN- β . Ovine IFN- τ binds to type I IFN receptors on cells with high affinity, but less strongly than IFN- α and IFN- β , to induce comparable anti-proliferative, antiviral and immunomodulatory activities [7,8]. A striking feature of IFN- τ is that it exhibits minimum or none cytotoxicity, even at high concentrations, compared to other members of interferon family [7]. *In vivo*, it has significantly lower toxicity than IFN- α and IFN- β when administered orally or by IV injections in pre-clinical or clinical studies [9-11]. Notably, IFN- τ has shown protective effects during pregnancy, and is important for the maternal recognition and maintenance of pregnancy in ruminants [12-14]. In mice it was shown to prevent embryo implantation failure [15]. In contrast, IFN- α and IFN- β exhibit severe toxicity in both animal and clinical studies, which include but not limited to tachycardia, nausea, weight loss, leucopenia, and neutropenia [16,17]. In a

Submitted: 07 October, 2023 | **Accepted:** 27 October, 2023 | **Published:** 30 October, 2023

***Corresponding author(s):** George Zhang, Ph.D. Southlake Pharmaceuticals, Inc, 125 Cambridge Park Drive, Cambridge, USA

Copyright: © 2023 Tang W, et al. This is an open-access article distributed under the terms of the Creative Commons Attribution License, which permits unrestricted use, distribution, and reproduction in any medium, provided the original author and source are credited.

Citation: Tang W, Liu X, Bazer FW, Zhang G (2023) Interferon Tau Is a Potent Oral Agent against SARS-CoV-2 Infection. SM J Infect Dis 6: 12.



head-to-head comparison study, significant levels of toxicity, such as severe decreases in lymphocytes, were detected in mice fed with IFN- α or IFN- β , but not with IFN- τ [7,9,16]. Another unique feature of IFN- τ is that it can be taken orally, unlike other members of interferon family, despite the mechanism of its oral activity is not fully understood. It was demonstrated that oral administration of IFN- τ increases energy metabolism, reduces adiposity, and alleviates inflammation of adipocytes and insulin resistance in rats and mice [18,19]. It was shown in a Ph2 clinical study in HCV patients that the oral treatment with IFN- τ at 15 mg/day for 84 days had some positive effect, and it was also safe and well tolerated [10].

IFN- α was previously reported to inhibit SARS-CoV-2 in Vero E6 cells *in vitro*. Pre-treatment with 1,000 U/mL recombinant IFN- α for 18 hours suppressed SARS-CoV-2 infection [20]. A previous study 21 on SARS-CoV mouse model suggested that the timing of the IFN response was influenced by viral load and age of the host. Low viral load induces early IFN responses, whereas high viral load and older hosts delay IFN responses. Early IFN response results in fast viral clearance and mild disease, while a delayed IFN response causes viral persistence, inflammation, and severe disease. Late onset of IFN response cannot control initial viral replication, but could cause inflammation and damage lungs instead [21,22]. It was observed in COVID-19 patients with severe infections, that there was a highly suppressed type I IFN response with little to no IFN production and activity [23]. These patients had a continuous viral burden in blood and an aggravated inflammatory response. It was suggested that the deficiency of type I IFN response is a hallmark of critical COVID-19 patients [23], and that type I IFN is beneficial for early-stage COVID-19 patients [24]. The need to explore dosing, timing and route of administration of type I IFNs at various stages of COVID-19 infection has been advocated, but the severe side effects of most type I interferons have limited this effort. Here we report, for the first time, that IFN- τ is effective in inhibiting COVID-19 infection in pre-clinical studies *in vitro* and *in vivo*, and it has an excellent safety profile compared to other type I interferons [25].

Results and Discussion

IFN- τ was previously shown to be effective as an oral agent in several metabolic disease models including those for diabetes, and obesity [18,19]. As a member of the type I interferon family, IFN- τ demonstrated promising anti-viral effects against human immunodeficiency virus and human papillomavirus [26-28]. Here we present data demonstrating that IFN- τ has remarkable anti-viral activity against SARS-CoV-2 virus. In a cellular CPE assay conducted in Vero E6 cells, IFN- τ potently inhibited SARS-CoV-2 activity with an IC_{50} of 2.1 nM (Figure 1A, 1B), which is 1,857 times more potent than Remdesivir (IC_{50} = 3.9 μ M), 910 times more potent than Hydroxychloroquine (IC_{50} = 1.91 μ M), 829 times more potent than Chloroquine (IC_{50} = 1.74 μ M), and 4667 times more potent than Aloxistatin (IC_{50} = 9.8 μ M) in the head-to-head comparison study (Figure 1C). The recently approved oral SARS-CoV-2 3-CL protease inhibitor, Paxlovid,

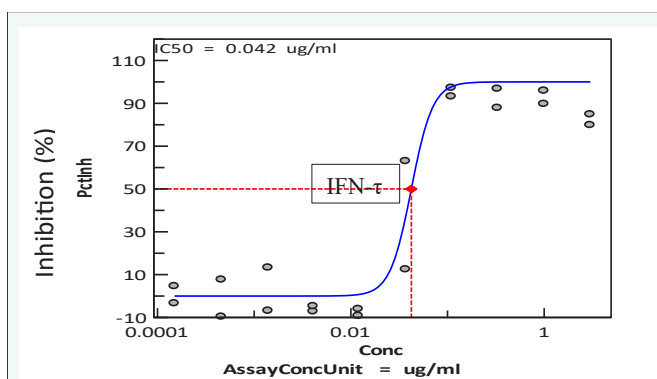


Figure 1a Anti-SARS-CoV2 Activity of IFN- τ in CPE assays with Vero E6 Cells.

Compounds were added to Vero E6 cells in a BSL2 lab, then the plates were taken to a BSL3 lab for viral inoculation. Cells were incubated for 72 hrs after viral inoculation before performing the CPE analyses. The assays were done in duplicates. Each dot represents one sample. IFN- τ potently inhibited SAR-CoV-2 activity with an IC_{50} of 2.1 nM (42 ng/ml).

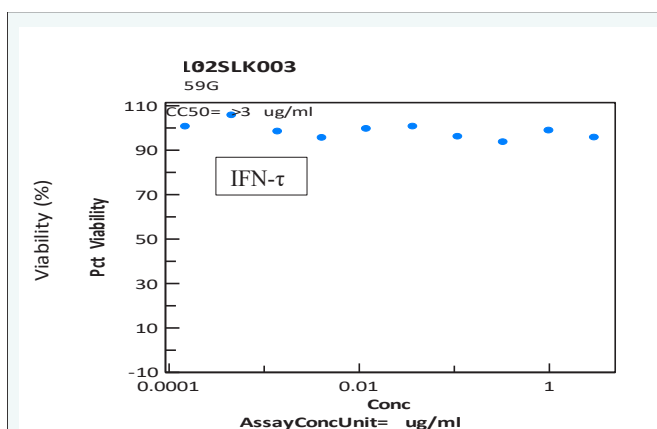


Figure 1b Effect of IFN- τ on viability of Vero E6 cells.

The viability of Vero E6 cells was determined using the CellTiter Glo (CTG) assay described in the Materials and Methods section. IFN- τ treatment did not affect viability of Vero E6 cells at concentrations tested up to 1 μ g/ml.

has an IC_{50} of 13 nM in the same assay, while Interferon λ has an IC_{50} of >150 nM (the highest concentration tested in the assay) (Figure 1C). It is, however, possible that different experimental designs, such as pre-treatment period, cell systems used, and variable viral titers and strains used in the experiment, could contribute to variable assay results. Cytotoxicity was evaluated for IFN- τ and the reference compounds in parallel with the CPE assays in host Vero E6 cells. For a direct comparison, the same 10 concentrations were used in the CPE assay. The cell viability was measured using Promega Cell Titer Glo with the CC_{50} values calculated using a four-parameter logistic fit. As shown in (Figure 1B), IFN- τ did not inhibit cell viability at all concentrations tested

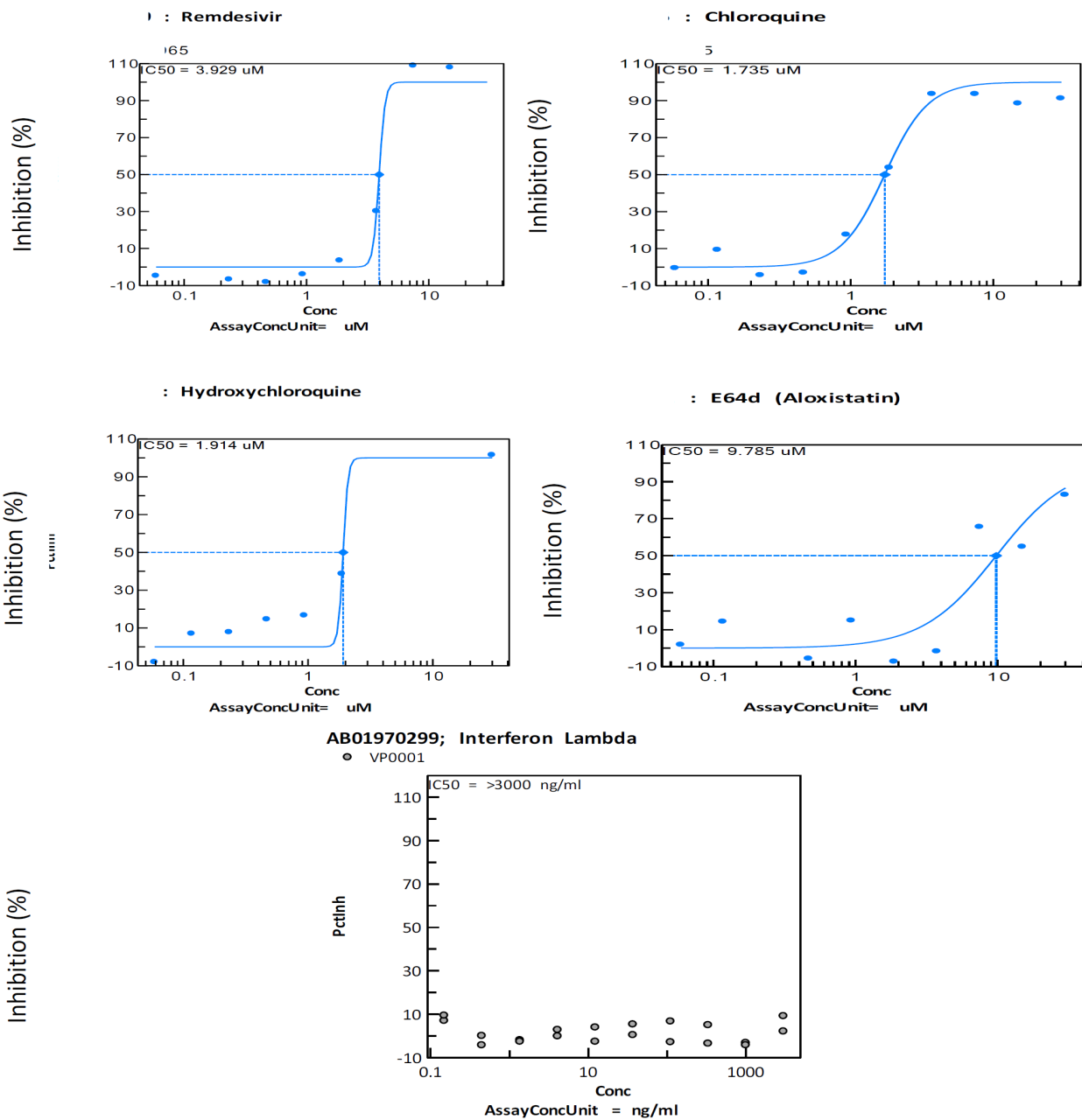


Figure 1c Anti-SARS-CoV2 Activity of Reference Compounds in CPE assays using Vero E6 cells.

The CPE assay for Vero E6 cells was performed as described for Figure 1A. Each dot represents one sample.

up to 150 nM (the highest concentration used in the assay).

We also performed SARS-CoV2 immunostaining assay using automated microscopy imaging in Calu-3 cells. The IC₅₀ of IFN- τ in this assay was 10.5 nM (Figure 2A), which is about 10 times more potent than Remdesivir (IC₅₀ = 99.4 nM) in the same assay (Figure 2B). The cytotoxicity of IFN- τ was also evaluated in this assay, and no evidence of cell toxicity was induced by either IFN- τ or Remdesivir treatment.

To evaluate the effect of IFN- τ on other types of coronaviruses, we conducted CPE assays for human coronaviruses hCoV-OC43 and hCoV-229E with IFN- τ and reference agents. IFN- τ did not exhibit anti-viral effects against hCoV-OC43 at the concentrations up to 1,000 ng/ml (the highest concentration tested), whereas the reference compound, Remdesivir, had an IC₅₀ of 41 nM in the assay. Chloroquine also had no significant effects against hCoV-OC43 with an IC₅₀ of 3,120 nM (Figure 3).

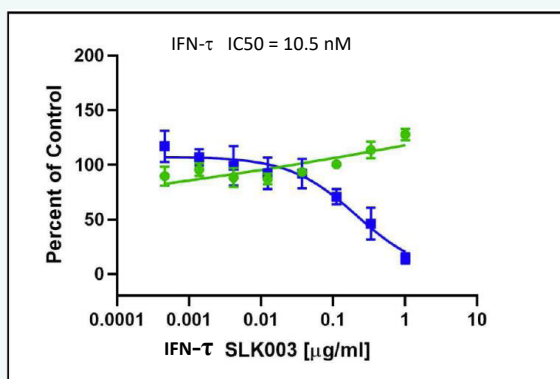


Figure 2a Anti-SARS-CoV2 Activity of IFN- τ in CPE assays using Calu-3 cells.

The CPE assays with Calu-3 cells was performed as described in the Materials and Methods section. Cells were incubated continuously with IFN- τ and SARS-CoV2 for 48 hours. Cells were fixed before being immunostained with anti-dsRNA (J2), and counterstaining nuclei with Hoechst 33342 for automated microscopy. The assay was performed in triplicate and error bars represent standard errors of the mean. The data were normalized to aggregated control wells and plotted versus IFN- τ to determine the IC_{50} (infection: blue) and CC_{50} (toxicity: green).

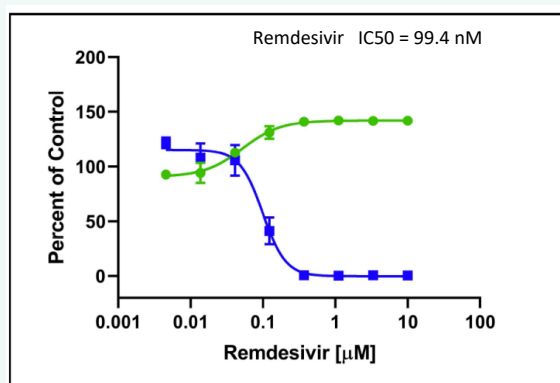


Figure 2b Anti-SARS-CoV2 Activity of Remdesivir in CPE assays using Calu-3 cells.

The CPE assay using Calu-3 cells was performed as described in the Materials and Methods section. Cells were incubated continuously with Remdesivir and SARS-CoV2 for 48 hours. Cells were fixed before being immunostained with anti-dsRNA (J2) and counterstaining nuclei with Hoechst 33342 for automated microscopy. The assay was performed in triplicate and error bars represent standard error of the mean. The data were normalized to aggregated control wells and plotted versus Remdesivir to determine the IC_{50} (infection: blue) and CC_{50} (toxicity: green).

For human coronavirus hCoV-229E, another respiratory disease-causing virus, IFN- τ potently inhibited its activity in the CPE assay. The IC_{50} of IFN- τ is 0.241 nM (Figure 4A), which is 100 times more potent than Remdesivir ($IC_{50} = 23.07$ nM) in the same assay (Figure 4B), and 10,000 times more potent than Chloroquine ($IC_{50} = 2.2$ μ M) (data not shown). The IC_{50} for Ribavirin, a nucleoside analogue and anti-viral agent approved

for treating chronic hepatitis C, is 30 μ M in this assay (data not shown). (Figure 4A) shows the lack of effect on cell viability treated with IFN- τ at all concentrations tested. These data provide the evidence that IFN- τ has potent activity against human coronaviruses SARS-CoV-2 and hCoV-229E, but not hCoV-OC43 in CPE assay *in vitro*. Compared to all reference compounds tested in the same assay, including Remdesivir, Chloroquine,

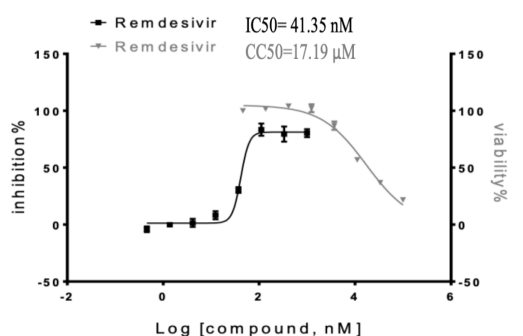
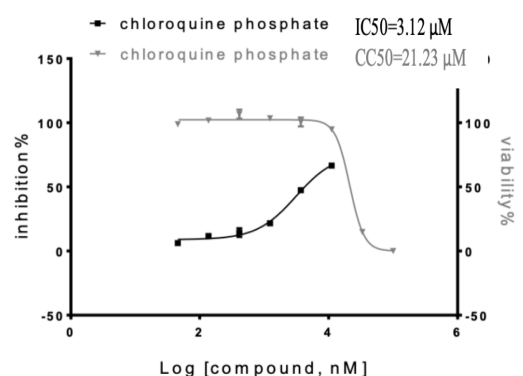
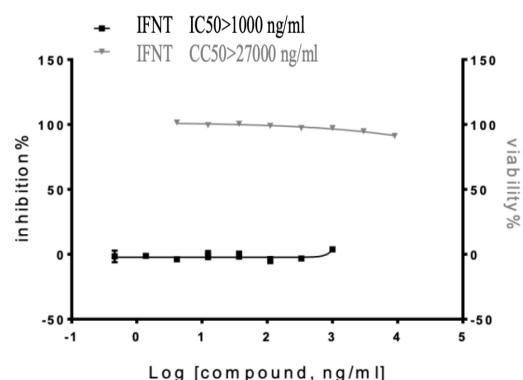


Figure 3 Anti-hCoV-OC43 Activity in CPE assay.

The CPE assays using Huh7 cells were performed as described in the Materials and Methods section. Cells were pre-treated with compounds for 24 hrs before virus inoculation, and then incubated for 7 days afterwards. Black dots and curves are dose-dependent inhibition curves. Grey dots and curves represent cell viability data. Error bars represent SEM (standard error of the mean).



Hydroxychloroquine, Aloxistatin, and Interferon λ , IFN- τ is significantly more potent against SARS-CoV-2 and CoV-229E viruses than other antiviral agents currently in use or at various stages of development for treating SARS-CoV-2 [29]. The lack of inhibition on hCoV-OC43 suggests that the anti-viral activity of IFN- τ is selective for certain types of coronaviruses. Although the reason for this selectivity is unknown, it might be due to the induction of the unique IFN-Inducible Transmembrane (IFITM) proteins reported to promote infection by hCoV-OC43 [30,31]. More importantly, IFN- τ had minimal cytotoxic effects in the cellular assays, which is consistent with the safety data reported in the previous phase I and II clinical trials [9,11], as well as in various animal studies *in vivo* [7,16].

We next studied the *in vivo* efficacy of oral administration of IFN- τ in a 9-10 week old BALB/c mouse model challenged with mouse-adapted SARS-CoV2 MA10 virus [32]. In this study, mice

were pre-treated with IFN- τ by oral gavage at 8 or 25 $\mu\text{g}/\text{kg}$ for 2 hr before viral challenge, and then dosed once a day for 2 or 5 days before the mice were euthanized at the end of the study (Day 2 or 5). The body weight change, clinical signs and viral load in lung tissues were then evaluated.

The mice challenged with the virus and treated with vehicle had an average decrease in body weight of 15%, whereas mice challenged with SARS-CoV-2 and treated with IFN- τ at 8 or 25 $\mu\text{g}/\text{kg}$ lost significantly less body weight than the vehicle control treated animals (Figure 5A). The improvement in body weight reduction did appear to carry over to improved clinical scores as mice from both IFN- τ groups (8 and 25 $\mu\text{g}/\text{kg}$) had similarly improved clinical scores between Study Day (SD) 2 and SD5 compared to the vehicle control group (Figure 5B).

Viral load analysis via qPCR indicated that oral administration

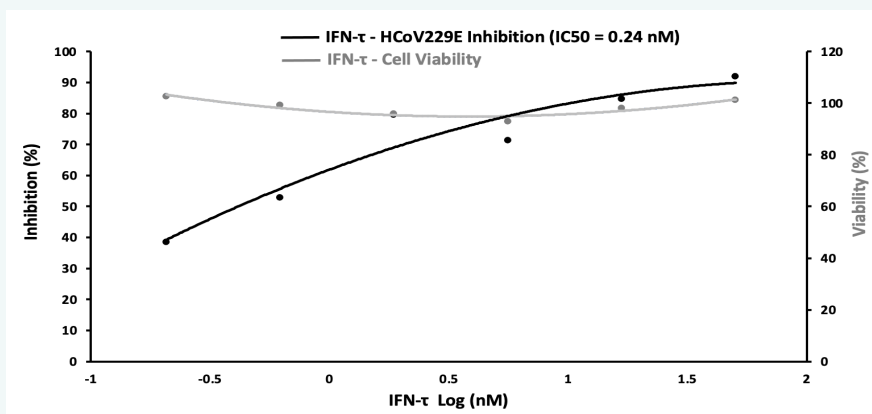


Figure 4a Anti-HCoV-229E activity of IFN- τ in CPE assays using MRC5 cells.

The CPE assays with MRC5 cells were performed as described in the Materials and Methods section. Cells were pre-incubated with IFN- τ for 2 hr before virus inoculation and incubated for 3 days afterwards. Samples were assayed in duplicates. The mean values are presented in the graphs.

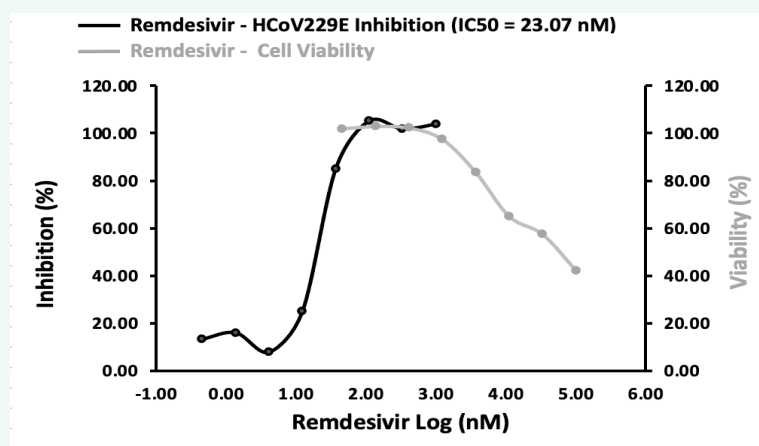


Figure 4b Anti-hCoV-229E Activity of Remdesivir in CPE assays using MRC5 cells.

The CPE assays with MRC5 cells were performed as described in the Materials and Methods section. Cells were pre-incubated with Remdesivir for 2 h before virus inoculation and incubated 3 days afterwards. Samples were assayed in duplicates with similar results. The mean values are presented in the graphs.

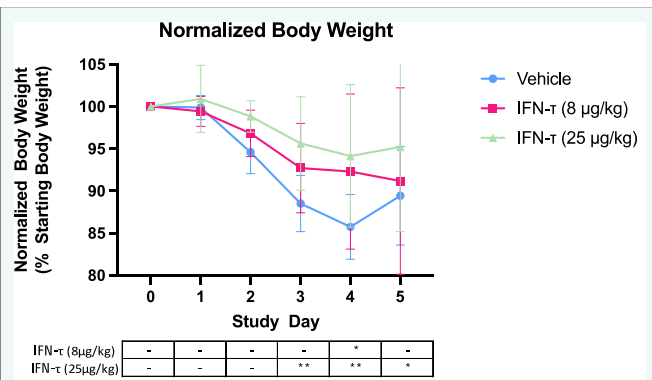


Figure 5a The Effect of IFN- τ on Changes in Body Weight of Mice in the Mouse Model for studies of SARS-CoV2.

Naïve female BALB/cAnNHsd mice at 11-12 weeks of age, were pre-treated with IFN- τ or Vehicle (PBS) for 2hrs before being inoculated intranasally with the mouse-adapted SARS-CoV-2 (MA10) virus. The virus challenge day is the Study Day (SD) 0. Mice were treated once a day with IFN- τ or PBS until being euthanized. Body weight was measured once each day. Data are presented as Mean \pm SEM. $**P < 0.01$, $*P < 0.05$. Statistical analysis using a main effects two-way ANOVA determined that there were significant differences in body weights between IFN- τ (25 μ g/kg) and Vehicle control mice on SD3, SD4 and SD5.

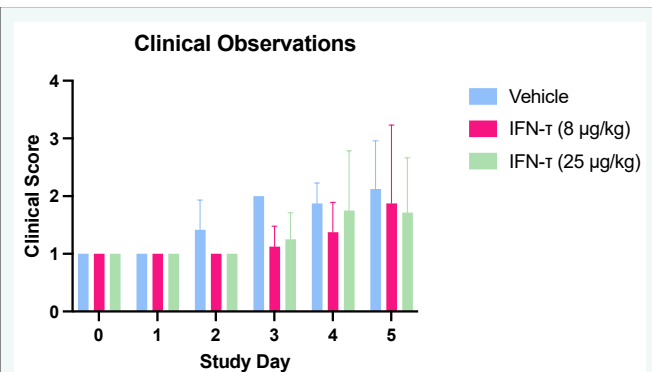


Figure 5b The Effect of IFN- τ on Clinical Scores for Mice in the Mouse Model of SARS-CoV2 study.

Mice were monitored at least once daily by visual examination. Clinical scoring and health assessments were performed and documented at each observation using the scoring system described in Material and Methods section. Data are presented as Mean \pm SEM.

of IFN- τ at 8 μ g/kg once a day suppressed viral load significantly ($P < 0.05$), and the viral load decreased about 10 times on SD2. For IFN- τ at 25 μ g/kg group on SD2, the viral RNA levels were suppressed about 10 times in 2 out of 4 mice in the group (Figure 5C). Although no statistically significant inhibitory effect on viral RNA by IFN- τ (25 μ g/kg) treatment on SD2, the mean value of this treatment group was lowered about 44%. The lack of statistical significance may be due to the low number of mice used in each group ($n = 4$). At the late stage of infection (SD5), both vehicle or IFN- τ -treated mice had lower viral RNA levels possibly due to spontaneous recovery of anti-viral immune response of the mice

in both groups by day 5 [33].

In addition, a statistically significant anti-viral activity was detected on SD2 as measured by TCID₅₀ (50% tissue culture infection dose) assay when mice were treated with oral IFN- τ at 25 μ g/kg (QD) when compared with the vehicle group (Figure 5D). The TCID₅₀ level was reduced more than 2 times by IFN- τ treatment at 25 μ g/kg (P.O., QD).

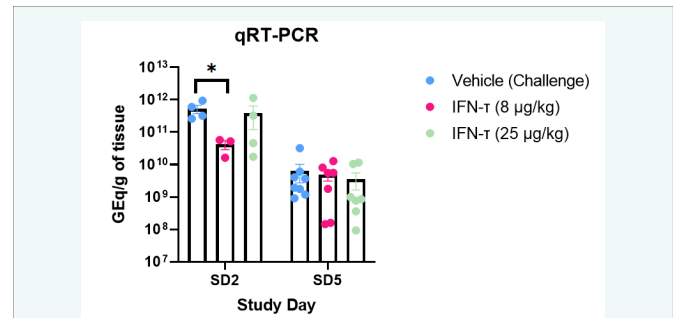


Figure 5c The Effect of IFN- τ on Viral Load as Assessed Using qPCR in the Mouse Model of SARS-CoV2.

(Outlier were excluded). Drug or vehicle was administered 2 h before virus inoculation, and then once a day until Study Day (SD) 2. After euthanasia, lungs were removed, homogenized and extracted for viral load analysis via qRT-PCR. Treatment groups are compared with the Vehicle (PBS) control group. Data on lung tissue are presented as Means \pm SEM, $*P < 0.05$. Statistical significance was analyzed by Student's t-test. One outlier in IFN- τ (8 μ g/kg) SD2 group and one in its SD 5 group were excluded according to Dixon's test for outlier on the following website: <https://contchart.com/outliers.aspx>. The graph was made by GraphPad Prism 9.3.1 software.

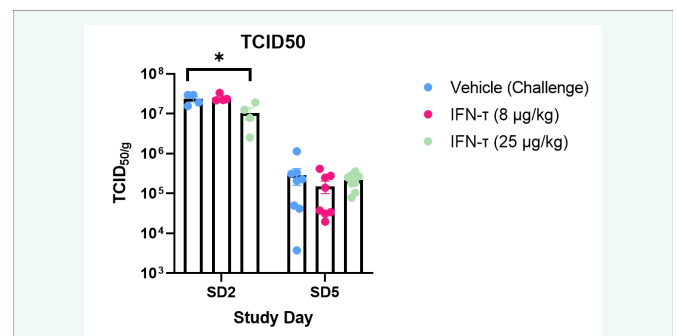


Figure 5d The Effect of IFN- τ on Viral Activity Assessed in a TCID₅₀ Assay in a Mouse Model of SARS-CoV2. Drug or vehicle was administered 2 h before virus inoculation, then once a day till Study Day 5. After euthanasia, lung tissues from mice were homogenized. Samples were serially, diluted 10-fold in MEM/2% Heat Inactivated-FBS for the TCID₅₀ assay. TCID₅₀ (The 50% of tissue culture infection dose) was determined based on tissue culture cytopathic effects as described in the Materials and Methods section. Viral load data are expressed as TCID₅₀ per gram of tissue. Data are presented as Means \pm SEM, $*P < 0.05$. Statistical significance was analyzed by Student's t-test.

TCID₅₀: The 50% tissue culture infection dose as determined by tissue culture cytopathic effects. The graph was made by GraphPad Prism 9.3.1 software.

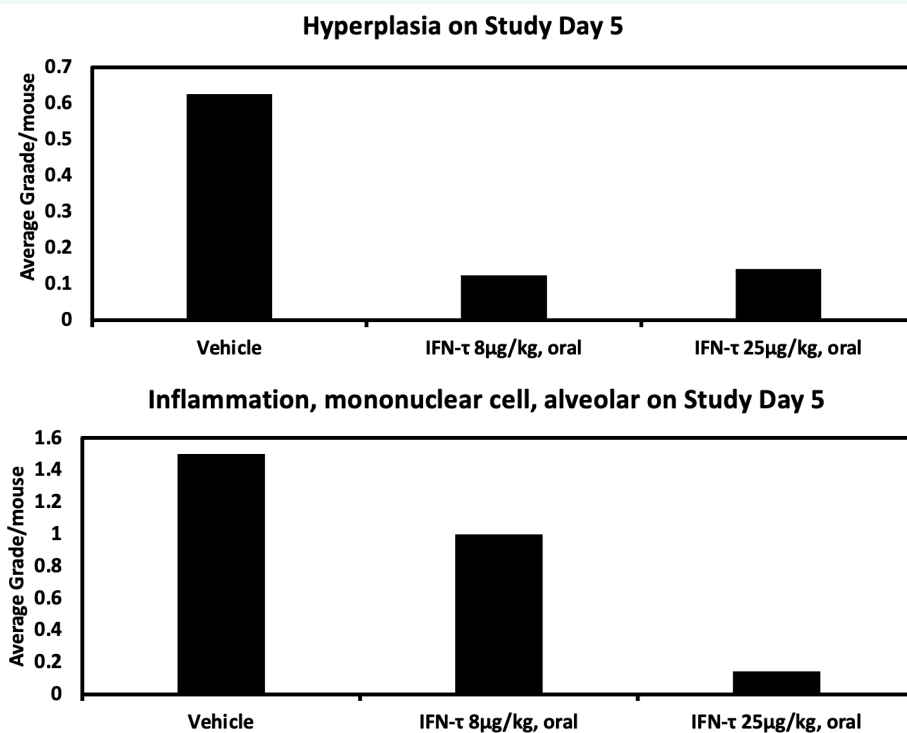


Figure 5e The Effect of IFN- τ on Lung Histopathology in a Mouse Model of SARS-CoV-2.

Mouse lung tissues were harvested and perfused with formalin and placed in 10% neutral buffered formalin for fixation after euthanasia on Study Day 5. Fixed tissues were processed to hematoxylin and eosin-stained slides and examined. The histopathology assay was performed as described in the Materials and Methods section with grades. From one to five according to severity. The severity of the non-neoplastic tissue lesions was graded as follows: Grade 1 is minimal, Grade 2 is mild, Grade 3 is moderate, Grade 4 is marked, Grade 5 is severe. The average grades per mouse for hyperplasia and inflammation in mononuclear cell and alveolar cells are presented in the graphs.

Histopathology analyses performed after completion of the study include macroscopic and microscopic findings. Macroscopic findings were observed in all groups on SD 2 and/or SD 5 and consisted of red, dark red, black, or light red spots. Hemorrhage, in most cases, was considered an artifact due to the presence of a tissue tear or separation. Due to equal incidence and severity of hemorrhage observed in all groups, this finding is probably unrelated to SARS-CoV-2 exposure or IFN- τ treatment. SARS-CoV-2-related microscopic findings in the lung on SD 2 included mixed or mononuclear cell alveolar, interstitial, peribronchial, and/or pleural inflammation; mononuclear cell perivascular inflammation; bronchial/bronchiolar epithelial necrosis/necrotic debris; interstitial necrotic debris; and/or alveolar necrotic debris. Necrosis and necrotic debris were observed early in SARS-CoV-2 infection. In this study, necrosis was greater at SD 2 than SD 5, as expected during the course of the disease.

The histopathology data on lung inflammation on SD5 demonstrated a slight decrease in incidence and severity of SARS-CoV-2-related microscopic findings in IFN- τ -treated mice as compared to the vehicle control mice (Figure 5E). Furthermore, both 8 μ g/kg and 25 μ g/kg IFN- τ alleviated the severity of

hyperplasia of lung tissues caused by viral infection. IFN- τ also decreased the severity of inflammation in mononuclear cells and alveoli cells in a dose-dependent manner.

In summary, our results demonstrate that IFN- τ has more potent anti-SARS-CoV-2 activity *in vitro* than other agents currently approved or in development for treating COVID-19 in a head-to-head comparison assay. The oral efficacy of IFN- τ in mice challenged with mouse-adapted SARS-CoV-2 virus was also demonstrated in our studies. Further, IFN- τ has well-documented excellent safety profile in previous pre-clinical and clinical studies compared to other type I interferons, such as IFN- α and - β . Taken together, IFN- τ is a potential effective and safe therapeutic candidate for treating COVID-19, and it may also serve as a prophylactic treatment agent due to its excellent safety profile. Clinical studies to verify efficacy and safety for COVID-19 treatment in human are warranted.

Materials and Methods

Anti-SARS-CoV-2 CPE assay in Vero E6 Cells

Materials: Most materials were purchased from commercial resources. Plates were Corning 3764 BC black-walled, clear bottom plates. Cell Titer Glo (CTG) was from Promega (G7573).



PBS $-/-$ (w/o Ca_2+ or Mg_2+), and media were purchased from Gibco: MEM (#11095) with 10% Heat Inactivated FBS Gibco (#14000). Trypsin-EDTA was also from Gibco (#25300-054). The study was with Vero E6 cells selected for high expression of ACE2 (angiotensin converting enzyme 2). Positive controls were Chloroquine (Southern Research Repository), Remdesivir, E64d (Selleck) and Hydroxychloroquine (Southern Research Repository).

Compounds: IFN- τ was supplied as stock solutions in Phosphate Buffered Saline (PBS) [18,19]. IFN- τ stock was stored at $-20^\circ C$ until the day of the assays. A set of positive control antiviral compounds were included in each of the assays performed. Interferon λ (Recombinant Human IL-29/IFN- λ 1, R&D Systems, Catalog Number: 1598-IL) was purchased as dry powder. Compound stocks were stored at $-20^\circ C$ until the day of the assays.

Virus Strains and Cell Lines: The virus strain (USA_WA1/2020) and cell line (Vero E6, ATCC Cat. No. CRL-1586) utilized in these studies were obtained from World Reference Center for Emerging Viruses and Arboviruses (WRCEVA) and American Type Culture Collection (ATCC), respectively. Vero E6 cells were selected for high expression of ACE2 (Angiotensin Converting Enzyme 2). Sorting and sub-cloning of Vero E6 cells for high expression of ACE2 was carried out. Cell culture medium was Dulbecco's Modified Eagle's Medium with 10% heat inactivated Fetal Bovine Serum and Amphotericin B. The assay medium was Dulbecco's Modified Eagle's Medium with 2% heat-inactivated Fetal Bovine Serum and 1% Penicillin and Streptomycin, and Amphotericin B. The analyses were A Cytopathic Effect (CPE) reduction assay to measure antiviral effects and a cell viability assay to determine cytotoxic effects of compounds.

On the day of each assay, a pre-titered aliquot of virus was taken from the freezer ($-80^\circ C$) and thawed to room temperature in a biological safety cabinet. The virus was re-suspended and diluted into Dulbecco's Modified Eagle's Medium (DMEM). Cells were sub-cultured twice each week at a split ratio of 1:2 to 1:5 using standard cell culture techniques. Total cell numbers and percent viability determinations were carried out using a Luna cell viability analyzer and trypan blue dye exclusion. Cell viability was greater than 95% for the cells used in the assays. There were 4000 cells seeded per well in a 384-well plate [34].

CPE Screening Procedure: a cell-based assay was utilized to measure the Cytopathic Effect (CPE) of the virus infecting Vero E6 host cells. The CPE reduction assay is used routinely and widely as an assay to screen for antiviral agents because of its ease of use in High Throughput Screening (HTS) [35,36]. In this assay, host cells infected with virus die because of the viral infection and an uncomplicated and robust cell viability assay is the readout. The CPE reduction assay indirectly monitors the effect of antiviral compounds functioning through various molecular mechanisms by measuring the viability of host cells 3 days after inoculation with the virus. Antiviral compounds are found as those that shielded the host cells from the cytopathic effects of the virus,

consequently enhancing cell viability. Positive controls were Chloroquine, Remdesivir, Hydroxychloroquine and E64d.

Preparation of Assay Ready Plates: IFN- τ stock solution supplied at 0.7 mg/ml in PBS was transferred into an Echo® Qualified 384-Well Polypropylene Source Microplate (Labcyte P-05525). IFN- τ was serially diluted 3-fold in PBS nine times. Employing a Labcyte ECHO 550 acoustic liquid handling system, a 127.5 nL aliquot of each diluted sample was dispensed into wells of a Corning 3764BC assay plate. This yielded a 235-fold dilution of each sample in a final assay volume of 30 μ L and provided the following final concentrations (μ g/mL) in the assay: 3.0, 1.0, 0.333, 0.111, 0.0370, 0.0123, 0.00412, 0.00137, 0.00046, 0.00015. IFN- τ was assayed in duplicates. Interferon λ was solubilized to 0.25 mg/ml with PBS. It was then diluted along with IFN- τ to 18 μ g/ml with media and serially diluted 3-fold in media nine times to give a 6x final assay concentration for assays. A 5 μ L aliquot of each diluted sample was transferred to assay ready plates to achieve final concentrations in assays as described previously. Interferon λ was assayed in duplicates. Positive controls were assayed with single sample and were assayed multiple times to achieve consistent results.

Method for measuring antiviral effects: The Vero E6 stable cell line expressing SARS-CoV2 receptor (ACE2; Angiotensin-Converting Enzyme 2) was used for the CPE assay [36]. Cells were grown in MEM/10% Heat Inactivated (HI) Fetal Bovine Serum (FBS) and harvested in MEM/1% PSG supplemented 2% HI FBS. Cells were batch inoculated with SARS-CoV2 (USA_WA1/2020) at M.O.I. (multiplicity of infection) \sim 0.002 to achieve approximately a 5% cell viability 72 hours post-infection. A 5 μ L aliquot of assay medium was dispensed into all wells of the assay plates, then the plates were transferred into the BSL-3 (Biosafety Level-3) facility. In the BSL-3 facility, a 25 μ L aliquot of virus was employed to inoculate cells (4000 Vero E6 cells/well) in each well in 22 columns, among which 2 columns of wells had only virus infected cells (no compound treatment). A 25 μ L aliquot of uninfected cells was dispensed to 2 columns of the assay plates for the cell only (no virus) controls. After incubating plates at $37^\circ C/5\%$ CO₂ and 90% humidity for 72 hours, 30 μ L of Cell Titer-Glo (Promega) was added to each well. Luminescence was read by a BMG CLARIOstar plate reader with MARS software following incubation at room temperature for 10 min to measure cell viability. Raw data from each test well were normalized to the average signal of non-infected cells (Avg Cells; 100% inhibition) and virus infected cells only (Avg Virus; 0% inhibition) to calculate percent inhibition of CPE using the following formula: percent inhibition CPE = $100 \times (\text{Test Compound} - \text{Avg Virus}) / (\text{Avg Cells} - \text{Avg Virus})$. Plates were sealed with a clear cover and the surface was decontaminated prior to luminescence reading.

Method for measuring cytotoxic effects of compounds: The cytotoxicity of compounds was analyzed using a BSL-2 counter screen with host cells in media being added in 25 μ L aliquots (4,000 cells/well) to each well of assay plates prepared with test compounds as described in the preceding section. Cells only



(100% viability) and cells treated with hyamine at 100 μ M final concentration (0% viability) were set as the high and low signal controls, respectively, for cytotoxic effects in the assay. After incubating plates at 37°C/5% CO₂ and 90% humidity for 72 h, plates were brought to room temperature and 30 μ l Cell Titer-Glo (Promega) was added to each well. Luminescence was read by a BMG PHERAstar plate reader after a 10 min incubation at room temperature to measure cell viability.

Data analysis: All raw data from plate readers were imported into ActivityBase wherein values were associated with compound Identifications (IDs) and test concentrations.

For the antiviral CPE reduction assay, raw signal values were converted to percent reduction in CPE using a standard formula [Percent CPE reduction = 100 x (test compound value – mean value for infected cells controls) / (mean value uninfected control cells – mean value for infected cell controls)].

For the cell viability assay to analyze compound cytotoxicity, percent cell viability was calculated using a standard formula [Percent viability = 100*(test compound value - mean low signal control) / (mean high signal control – mean low signal control)]. IC₅₀ and CC₅₀ values were calculated using a four-parameter logistic fit of data using the Xlfit module of ActivityBase.

Anti-SARS-CoV-2 Assay Using Calu-3 Cells

Briefly, Calu-3 cells (ATCC, HTB-55) were cultured in Minimal Eagles Medium supplemented with 0.1% non-essential amino acids, 0.1% penicillin/streptomycin, and 10% FBS. Cells were plated in 384 well plates. The next day, 50 nL of IFN- τ suspended in PBS was added as an 8-point dose response with three-fold dilutions between test concentrations in triplicate, starting at 1 μ g/ml concentration. The concentrations (μ g/mL) tested were: 1.0, 0.333, 0.111, 0.0370, 0.0123, 0.00412, 0.00137, and 0.00046. The negative control (PBS, n = 32) and positive control (10 μ M Remdesivir, n = 32) were included on each assay plate. Calu-3 cells were pretreated with control compounds and IFN- τ (in triplicate) for 2 h prior to infection. In a BSL3 lab, SARS-CoV-2 (isolate USA WA1/2020), diluted in serum free growth medium, was dispensed to plates to achieve an MOI = 0.5. Cells were incubated continuously with IFN- τ and SARS-CoV2 for 48 h. Cells were fixed and then immunostained with anti-dsRNA (J2) and nuclei were counterstained with Hoechst 33342 for automated microscopy.

Automated image analysis quantified the number of cells per well (toxicity) and the percentage of infected cells (dsRNA+ cells/cell number) per well. Data were normalized to aggregated PBS control well data and plotted versus IFN- τ concentration to determine the IC₅₀ (for infection), and CC₅₀ (for toxicity). These values are presented for IFN- τ tested along with the positive control (Remdesivir).

Anti-hCoV-OC43 CPE Assay

The method for the anti-hCoV-OC43 CPE assay was with test samples and reference compounds at eight concentrations

with 3-fold dilutions starting at 1,000 ng/ml in duplicates. In 96-well plates, Huh7 cells were seeded at an appropriate density and cultured at 37°C and 5% CO₂ for 4-6 hours. Test samples were dispensed into wells and the plates were incubated at 37°C and 5% CO₂ for 24 h. Then medium in each well was replenished with medium containing serially diluted samples/reference compounds and virus (300 TCID₅₀ hCoV-OC43 vs 8,000 Huh7 cells). The resulting cultures were kept under the same conditions for an additional 7 days until virus infection in the virus control induced a significant CPE. Cytotoxicity of the compounds was analyzed under the same conditions, but without virus infection, in parallel. Test samples and reference compounds were evaluated at eight concentrations with 3-fold dilutions starting at 27,000 ng/mL in duplicates. Cell viability was measured by CellTiter Glo following the manufacturer's instructions. Luminescence was read by a Synergy 2 (BioTek) plate reader with GEN5.1.08 software. The IC₅₀ and CC₅₀ values were calculated using GraphPad Prism software [37].

Anti-hCoV-229E CPE Assay

For the Anti-hCoV-229E CPE assay, MRC5 cells were seeded at an appropriate density and cultured at 37°C and 5% CO₂ overnight in 96-well plates. Test samples were added into wells and the plates were incubated at 37°C and 5% CO₂ for 2 h. Then medium in each well was replenished with medium containing serially diluted samples and virus (200 TCID₅₀ hCoV-229E vs 20,000 MRC5 cells). The resulting cultures were kept under the same conditions for additional 3 days until virus infection in the virus control cells induced a significant CPE. Cytotoxicity of the compounds was analyzed in duplicates under the same conditions, but without virus infection, in parallel. Cell viability was measured by CellTiter Glo following the manufacturer's instructions. Luminescence was read by Synergy 2 (BioTek) plate reader with GEN5.1.08 software. The IC₅₀ and CC₅₀ values were calculated using GraphPad Prism software. Samples were assayed in duplicates. The experiment was repeated twice with similar results.

Anti-SARS-CoV2 *In vivo* Efficacy Study

Animals: Thirty-six (36) female BALB/cAnNHsd mice were purchased from Envigo. They were of 9-10 weeks old at time of delivery and were of 11-12 weeks old at the time of viral challenge. Mice were housed in the University of Texas Medical Branch Animal Facility. All animal handling and experiments were carried out according to the provisions of the Animal Welfare Act, PHS Animal Welfare Policy, the principles of the NIH Guide for the Care and Use of Laboratory Animals, and the policies and procedures of the University of Texas Medical Branch (UTMB). This study was conducted in UTMBs AAALAC (Association for the Assessment and Accreditation of Laboratory Animal Care)-accredited facilities and were approved by the Institutional Animal Care and Use Committee (IACUC).

Treatment: IFN- τ , provided by Southlake Pharmaceuticals at a concentration of 1.5 mg/mL, was prepared fresh daily at



concentrations of 8 and 25 µg/kg using an average mouse weight of 20g for dose calculations. Beginning 2 hours prior to challenge on SD0, mice were anesthetized and treated via oral gavage with 50 µL of vehicle (Group 1) or IFN-τ at the appropriate concentrations (Groups 2 and 3).

Challenge: This study was performed at UTMB under Biosafety Level 3 conditions. The thirty-six (36) experimentally naïve mice (11-12 weeks old at time of challenge) were divided into three groups: Vehicle (Group 1; n = 12), IFN-τ 8 µg/kg (Group 2; n = 12) and IFN-τ 25 µg/kg (Group 3; n = 12). Each group was administered 1.0×10^5 TCID₅₀ SARS-CoV-2 (MA10) intranasally in a volume of 60 µL (30 µL per nare). The mouse-adapted SARS-CoV-2 (MA10) virus was supplied by UTMB. Mice were monitored daily for alterations in activity, behavior, appearance, and body weight. Body weights were normalized to each mouse starting body weight collected on SD0 prior to treatment. Scheduled euthanasia events occurred on SD2 and SD5. The lungs from each mouse were removed, weighed, and examined for SARS-CoV-2 viral loads and histopathology. For viral load analysis, the left lung lobe was homogenized in 500 µL of PBS, centrifuged and the resulting supernatant was analyzed for infectious virus via TCID₅₀ assay and for genomic viral RNA by qRT-PCR. Virus challenge day was defined as study day (SD) 0. Stock virus was removed from frozen storage and allowed to thaw under ambient conditions. The thawed suspension was diluted in Minimum Essential Medium (MEM) to a target challenge dose concentration of 1.7×10^6 TCID₅₀/mL, such that animals received a target of 1.0×10^5 TCID₅₀ per 60 µL dose. Virus administration was performed intranasally (i.n.) with 30 µL being administered into each nare. In each group, 4 mice were sacrificed on Study Day 2 (SD2), and 8 mice were sacrificed on SD5.

Viral Load Determination

From each animal scheduled for euthanasia, representative samples of lung tissue were collected for viral load analysis. Upon collection, tissue was placed into an Eppendorf tube containing sterile phosphate buffered saline and 1-2 x 5 mm sterile stainless-steel beads. Tissue samples were homogenized using a QIAGEN TissueLyser. Following homogenization, samples were clarified via centrifugation. Clarified supernatant was stored frozen ($\leq -65^\circ\text{C}$) after removal of the aliquot for RNA extraction (see below).

qRT-PCR: Clarified lung homogenate (50 µL) was added to TRIzol® LS Reagent (250 µL) and allowed to incubate under ambient conditions for 10 minutes. Samples were processed to RNA using Zymo Direct-zol™ RNA Miniprep kits. (Zymo Research, Irvine, CA, USA) per manufacturer instructions. RNA samples were analyzed via qRT-PCR targeting the SARS-CoV-2 E gene to detect genomic RNA. The probe (Integrated DNA Technologies, Coralville, IA, USA) was labeled at the 5'-end with fluorophore 9-carboxyfluorescein (6-FAM) and included an internal quencher (ZEN) and a 3'-end quencher (IowaBlackFQ, IABkFQ). The master mix was prepared by combining forward primer (250 nM, 5'-ACA GGT ACG TTA ATA GTT AAT AGC GT-

3'), reverse primer (250 nM, 5'-ATA TTG CAG CAG TAC GCA CAC A-3'), and probe (375 nM, 5'-6FAM-ACA CTA GCC/ZEN/ATC CTT ACT GCG CTT CG-IABkFQ-3') with 12.5 µL of 2X QuantiFast Probe Mix (QIAGEN, Germantown, MD, USA), 0.25 µL of 2X QuantiFast RT Mix (QIAGEN), and PCR-grade water (fill to 20 µL). A test sample (5 µL) was added to the master mix, resulting in a final volume of 25 µL per reaction. Real-time analysis was performed using the Bio-Rad CFX96™ Real-Time PCR Detection System. Thermocycling conditions were as follows: step 1, 1 cycle, 50°C for 10 min; step 2, 1 cycle, 95°C for 10 min; steps 3-5, 45 cycles, 95°C for 10 s, 60°C for 30 s, single read. Negative controls included reaction mixtures without RNA. For quantification purposes, a serial diluted synthetic oligonucleotide was used to generate the standard curve. All qRT-PCR results are expressed as GEq/g of tissue.

TCID₅₀: Infectious SARS-CoV-2 was measured by TCID₅₀ analysis as in a previous publication [37]. Samples were frozen immediately after homogenization. Prior to analysis, samples were removed from frozen storage and allowed to thaw under ambient conditions. Samples were serially diluted and incubated on Vero C1008 (E6) cells (BEI Resources, NR-596, Lot 3956593) in 96 well plates with negative and positive control. The plates were incubated for 96 hours when cytopathic effect (CPE) was measured by microscopic observation. All TCID₅₀ results are expressed as TCID₅₀/g of tissue.

Two-way ANOVA was used to determine differences among groups followed by a Tukey's multiple comparison test. Student's t-test was used to determine differences between two groups.

Clinical Observation

Animals were monitored visually at least once daily as were body weight. Clinical scoring and health assessments were performed and documented during each observation using the following scoring system: Score 1 is healthy and no further observation is required; Score 2 means ruffled fur, being lethargic and no further observation is required; Score 3 has Score 2's appearance plus one additional sign such as: hunched posture, orbital tightening, labored breathing/dyspnea, reduced mobility/movement, and 2nd observation is required; Score 4 shows reluctance to move when stimulated and immediate euthanasia is required.

Once mice reached a clinical score of 3, they were observed twice daily with 6-8 hours between observations. All surviving mice were humanely euthanized on Study Day 5.

Mice were weighed daily beginning on SD0 prior to test article administration. Mice that reached or exceeded a body weight loss of 20% were immediately euthanized. Scheduled euthanasia events occurred on SD2, and SD5. During the scheduled necropsy, the lungs were removed for viral load analyses using qRT-PCR, TCID₅₀, and histopathology (H&E staining). Lungs collected for viral load determination were weighed.

Body weights were normalized to each animals starting



body weight collected on SD0 prior to treatment. Scheduled euthanasia events occurred on SD2 and SD5. The lungs from each mouse were removed, weighed, and examined for SARS-CoV-2 viral loads and histopathology. For viral load analysis, the left lung lobe was homogenized in 500 μ L of PBS, centrifuged and the resulting supernatant was analyzed for infectious virus via TCID₅₀ assay and for genomic viral RNA by qRT-PCR.

Histopathology

For each animal scheduled for euthanasia, representative sections of lung tissue were collected for histopathological analysis. Tissues were collected on all euthanized animals. Upon collection, tissues were perfused with formalin and placed in 10% neutral buffered formalin for fixation. Fixed tissues were processed to hematoxylin and eosin-stained slides and examined by a board-certified pathologist at Experimental Pathology Laboratories, Inc. (EPL®) in Sterling, Virginia. Histopathology findings include macroscopic findings and microscopic findings.

Acknowledgment

We appreciate the University of Pennsylvania High Throughput Core for carrying out the anti-SARS-CoV2 assay with Calu-3 cells. Work performed at the University of Texas Medical Branch was funded in whole or in part with Federal funds from the National Institute of Allergy and Infectious Diseases, National Institutes of Health, Department of Health and Human Services, under Contract No. HHSN272201700040I. We appreciate the experimental services by Southern Research (Birmingham, AL) for performing the anti-SARS-CoV2 CPE assay in Vero E6 cells; and WuXi AppTec (Shanghai, China) for carrying out anti-hCoV-229E and anti-hCoV-OC43 CPE assays.

Author Contributions

Wanjin Tang, George Zhang and Xiaojun Liu conceived and designed the studies. Wanjin Tang, George Zhang, Fuller W Bazer and Xiaojun Liu, drafted the paper.

References

1. Sanders JM, Monogue ML, Jodlowski TZ, Cutrell JB. Pharmacologic Treatments for Coronavirus Disease 2019 (COVID-19): A Review. *JAMA*. 2020; 323(18): 1824-1836. doi: 10.1001/jama.2020.6019. PMID: 32282022.
2. Mahase E. Covid-19: Remdesivir is helpful but not a wonder drug, say researchers. *BMJ*. 2020; 369: m1798. doi: 10.1136/bmj.m1798. PMID: 32357949.
3. Mahase E. Covid-19: Remdesivir probably reduces recovery time, but evidence is uncertain, panel finds. *BMJ*. 2020; 370: m3049. doi: 10.1136/bmj.m3049. PMID: 32732277.
4. Juurlink DN. Safety considerations with chloroquine, hydroxychloroquine and azithromycin in the management of SARS-CoV-2 infection. *CMAJ*. 2020; 192(17): E450-E453. doi: 10.1503/cmaj.200528. Epub 2020 Apr 8. Erratum in: *CMAJ*. 2020 May 25;192(21):E590. PMID: 32269021; PMCID: PMC7207200.

5. Roustit M, Guilhaumou R, Molimard M, Drici MD, Laporte S, Montastruc JL, et al. Chloroquine and hydroxychloroquine in the management of COVID-19: Much kerfuffle but little evidence. *Therapie*. 2020; 75(4): 363-370. doi: 10.1016/j.therap.2020.05.010. Epub 2020 May 23. PMID: 32473812; PMCID: PMC7244425.
6. Bazer FW, Spencer TE, Ott TL. Placental interferons. *Am J Reprod Immunol*. 1996; 35(4): 297-308. doi: 10.1111/j.1600-0897.1996.tb00485.x. PMID: 8739445.
7. Soos JM, Subramaniam PS, Hobeika AC, Schiffenbauer J, Johnson HM. The IFN pregnancy recognition hormone IFN-tau blocks both development and superantigen reactivation of experimental allergic encephalomyelitis without associated toxicity. *J Immunol*. 1995; 155(5): 2747-53. PMID: 7544384.
8. Pontzer CH, Bazer FW, Johnson HM. Antiproliferative activity of a pregnancy recognition hormone, ovine trophoblast protein-1. *Cancer Res*. 1991; 51(19): 5304-5307. PMID: 1913653.
9. Jeanne M. Soos, Joel Schiffenbauer, Howard Marcellus Johnson. Orally Administered Interferon Tau Compositions and Methods. US 6,372,206 B1. 2002.
10. Chih-Ping Liu, Lorelie H Villarete, Stephen N Kirnon. Method of Optimizing Treatment with Interferon-Tau. USA patent (PCT/US2005/008314). 2005.
11. Waubant E. Emerging therapies for MS. *Rev Neurol (Paris)*. 2007; 163(6-7): 688-696. doi: 10.1016/s0035-3787(07)90481-6. PMID: 17607191.
12. Basavaraja R, Madusanka ST, Drum JN, Shrestha K, Farberov S, Wiltbank MC, et al. Interferon-Tau Exerts Direct Prosurvival and Antiapoptotic Actions in Luteinized Bovine Granulosa Cells. *Sci Rep*. 2019; 9(1): 14682. doi: 10.1038/s41598-019-51152-6. PMID: 31605002; PMCID: PMC6789004.
13. Brooks K, Spencer TE. Biological roles of interferon tau (IFNT) and type I IFN receptors in elongation of the ovine conceptus. *Biol Reprod*. 2015; 92(2): 47. doi: 10.1095/biolreprod.114.124156. Epub 2014 Dec 10. PMID: 25505203.
14. Bazer FW, Ying W, Wang X, Dunlap KA, Zhou B, Johnson GA, et al. The many faces of interferon tau. *Amino Acids*. 2015; 47(3): 449-460. doi: 10.1007/s00726-014-1905-x. Epub 2015 Jan 4. PMID: 25557050.
15. Jiang K, Yang J, Chen Y, Guo S, Zhao G, Wu H, et al. Protective Effects of Interferon-tau Against Lipopolysaccharide-Induced Embryo Implantation Failure in Pregnant Mice. *J Interferon Cytokine Res*. 2018; 38(5): 226-234. doi: 10.1089/jir.2017.0126. Epub 2018 May 3. PMID: 29723118.
16. Degré M. Influence of exogenous interferon on the peripheral white blood cell count in mice. *Int J Cancer*. 1974; 14(6): 699-703. doi: 10.1002/ijc.2910140602. PMID: 4463167.
17. Karl Fent, Gerhard Zbinden. Toxicity of interferon and interleukin. *Trends in Pharmacological Sciences*. 1987; 8(3): 100-105.
18. Tekwe CD, Lei J, Yao K, Rezaei R, Li X, Dahanayaka S, et al. Oral



- administration of interferon tau enhances oxidation of energy substrates and reduces adiposity in Zucker diabetic fatty rats. *Biofactors*. 2013; 39(5): 552-563. doi: 10.1002/biof.1113. Epub 2013 Jun 27. PMID: 23804503; PMCID: PMC3786024.
19. Ying W, Kanameni S, Chang CA, Nair V, Safe S, Bazer FW, et al. Interferon tau alleviates obesity-induced adipose tissue inflammation and insulin resistance by regulating macrophage polarization. *PLoS One*. 2014; 9(6): e98835. doi: 10.1371/journal.pone.0098835. PMID: 24905566; PMCID: PMC4048269.
20. Kumari G Lokugamage, Adam Hage, Maren de Vries, Ana M Valero-Jimenez, Craig Schindewolf. SARS-CoV-2 is sensitive to type I interferon pretreatment. *bioRxiv*. 2020; doi:10.1101/2020.03.07.982264.
21. Channappanavar R, Fehr AR, Vijay R, Mack M, Zhao J, Meyerholz DK, et al. Dysregulated Type I Interferon and Inflammatory Monocyte-Macrophage Responses Cause Lethal Pneumonia in SARS-CoV-Infected Mice. *Cell Host Microbe*. 2016; 19(2): 181-193. doi: 10.1016/j.chom.2016.01.007. PMID: 26867177; PMCID: PMC4752723.
22. Park A, Iwasaki A. Type I and Type III Interferons - Induction, Signaling, Evasion, and Application to Combat COVID-19. *Cell Host Microbe*. 2020; 27(6): 870-878. doi: 10.1016/j.chom.2020.05.008. Epub 2020 May 27. PMID: 32464097; PMCID: PMC7255347.
23. Hadjadj J, Yatim N, Barnabei L, Corneau A, Boussier J, Smith N, et al. Impaired type I interferon activity and inflammatory responses in severe COVID-19 patients. *Science*. 2020; 369(6504): 718-724. doi: 10.1126/science.abc6027. Epub 2020 Jul 13. PMID: 32661059; PMCID: PMC7402632.
24. Wadman M. Can interferons stop COVID-19 before it takes hold? *Science*. 2020; 369(6500): 125-126. doi: 10.1126/science.2020.6500.369_125. PMID: 32646977.
25. Aricò E, Bracci L, Castiello L, Gessani S, Belardelli F. Are we fully exploiting type I Interferons in today's fight against COVID-19 pandemic? *Cytokine Growth Factor Rev*. 2020; 54: 43-50. doi: 10.1016/j.cytogfr.2020.07.010. Epub 2020 Jul 4. PMID: 32665127; PMCID: PMC7334951.
26. Dereuddre-Bosquet N, Clayette P, Martin M, Mabondzo A, Frétier P, Gras G, et al. Anti-HIV potential of a new interferon, interferon-tau (trophoblastin). *J Acquir Immune Defic Syndr Hum Retrovirol*. 1996; 11(3): 241-246. doi: 10.1097/00042560-199603010-00004. PMID: 8603260.
27. Fujii Y, Murase Y, Otake K, Yokota Y, Omoto S, Hayashi H, et al. A potential live vector, foamy virus, directed intra-cellular expression of ovine interferon-tau exhibited the resistance to HIV infection. *J Vet Med Sci*. 2004; 66(2): 115-121. doi: 10.1292/jvms.66.115. PMID: 15031537.
28. Johnson JA, Hochkeppel HK, Gangemi JD. IFN-tau exhibits potent suppression of human papillomavirus E6/E7 oncoprotein expression. *J Interferon Cytokine Res*. 1999; 19(10): 1107-1116. doi: 10.1089/107999099313046. PMID: 10547150.
29. Madonov PG, Svyatchenko VA, Legostaev SS, Kikhtenko NA, Kotlyarova AA, Oleinik LA, et al. Evaluation of the Anti-Viral Activity of Human Recombinant Interferon Lambda-1 against SARS-CoV-2. *Bull Exp Biol Med*. 2021; 172(1): 53-56. doi: 10.1007/s10517-021-05330-0. Epub 2021 Nov 18. PMID: 34791556; PMCID: PMC8598276.
30. Zhao X, Guo F, Liu F, Cuconati A, Chang J, Block TM, et al. Interferon induction of IFITM proteins promotes infection by human coronavirus OC43. *Proc Natl Acad Sci U S A*. 2014; 111(18): 6756-6761. doi: 10.1073/pnas.1320856111. Epub 2014 Apr 21. PMID: 24753610; PMCID: PMC4020042.
31. Martín V, Pascual E, Avia M, Rangel G, de Molina A, Alejo A, et al. A Recombinant Adenovirus Expressing Ovine Interferon Tau Prevents Influenza Virus-Induced Lethality in Mice. *J Virol*. 2016; 90(7): 3783-3738. doi: 10.1128/JVI.03258-15. PMID: 26739058; PMCID: PMC4794696.
32. Dinnon KH 3rd, Leist SR, Schäfer A, Edwards CE, Martinez DR, Montgomery SA, et al. A mouse-adapted model of SARS-CoV-2 to test COVID-19 countermeasures. *Nature*. 2020; 586(7830): 560-566. doi: 10.1038/s41586-020-2708-8. Epub 2020 Aug 27. Erratum in: *Nature*. 2021 Feb;590(7844):E22. PMID: 32854108; PMCID: PMC8034761.
33. Asselin E, Johnson GA, Spencer TE, Bazer FW. Monocyte chemotactic protein-1 and -2 messenger ribonucleic acids in the ovine uterus: regulation by pregnancy, progesterone, and interferon-tau. *Biol Reprod*. 2001; 64(3): 992-1000. doi: 10.1095/biolreprod64.3.992. PMID: 11207217.
34. Fleming JA, Song G, Choi Y, Spencer TE, Bazer FW. Interferon regulatory factor 6 (IRF6) is expressed in the ovine uterus and functions as a transcriptional activator. *Mol Cell Endocrinol*. 2009; 299(2): 252-260. doi: 10.1016/j.mce.2008.10.025. Epub 2008 Oct 30. PMID: 19022341; PMCID: PMC2655364.
35. Maddox CB, Rasmussen L, White EL. Adapting Cell-Based Assays to the High Throughput Screening Platform: Problems Encountered and Lessons Learned. *JALA Charlottesville Va*. 2008; 13(3): 168-173. doi: 10.1016/j.jala.2008.02.002. PMID: 19492073; PMCID: PMC2673009.
36. Severson WE, Shindo N, Sosa M, Fletcher T 3rd, White EL, Ananthan S, et al. Development and validation of a high-throughput screen for inhibitors of SARS CoV and its application in screening of a 100,000-compound library. *J Biomol Screen*. 2007; 12(1): 33-40. doi: 10.1177/1087057106296688. Epub 2006 Dec 22. PMID: 17200104; PMCID: PMC9050465.
37. Chan CEZ, Seah SGK, Chye H, Massey S, Torres M, Lim APC, et al. The Fc-mediated effector functions of a potent SARS-CoV-2 neutralizing antibody, SC31, isolated from an early convalescent COVID-19 patient, are essential for the optimal therapeutic efficacy of the antibody. *PLoS One*. 2021; 16(6): e0253487. doi: 10.1371/journal.pone.0253487. PMID: 34161386; PMCID: PMC8221499.